m^{6}A-mediated LINC02038 inhibits colorectal cancer progression via regulation of the FAM172A/PI3K/AKT pathway via competitive binding with miR-552-5p

WENJUN LIU[1*], ZILANG ZHANG[2*], XITU LUO[1], KAI QIAN[3], BAOJUN HUANG[1], JIANMIN LIANG[1], ZHIHAO MA[1], JIANZHONG DENG[2] and CHENGYU YANG[1]

[1]The First Department of General Surgery, The Third Affiliated Hospital of Guangzhou Medical University, Guangzhou, Guangdong 510150; [2]Department of AnoRectal Surgery, The First People's Hospital of Foshan, Foshan, Guangdong 528010; [3]Division of Vascular and Interventional Radiology, Department of General Surgery, Nanfang Hospital, Southern Medical University, Guangzhou, Guangdong 510000, P.R. China

Received January 31, 2023; Accepted May 18, 2023

DOI: 10.3892/ijo.2023.5529

Abstract. Long noncoding RNAs (lncRNAs) are a type of regulatory molecule with potential roles in the development of several different malignancies. However, the underlying mechanisms of lncRNAs in colorectal cancer (CRC) are incompletely understood. The present study investigated the molecular mechanism of LINC02038 in CRC. LINC02038 expression was decreased in CRC tissues compared to the para-cancerous tissues and LINC02038 overexpression markedly reduced the proliferation, vitality, migration and invasive ability and greatly accelerated apoptosis of colorectal cancer cells. Bioinformatics examination indicated that LINC02038 may have targeted microRNA (miR)-552-5p. RNA immunoprecipitation and luciferase reporter assays showed that LINC02038 served as a sponge for miR-552-5p, hindering target gene FAM172A of miR-552-5p degradation. Moreover, methylated RNA immunoprecipitation (MeRIP)-qualitative PCR assays revealed that YTHDF2 could identify and regulate the METTL3-mediated LINC02038 N6-methyladenosine (m^{6}A) modification and increase its degradation, thereby promoting CRC progression via the PI3K/AKT pathway. Based on the CRC clinical specimens, it was shown that LINC02038 was negatively associated with lymphatic metastasis and distant metastasis. These results revealed that m^{6}A/LINC02038/miR-552-5p/FAM172A may be a novel anti-tumor axis and LINC02038 may serve as a biomarker and treatment option for colorectal cancer.

Correspondence to: Dr Chengyu Yang, The First Department of General Surgery, The Third Affiliated Hospital of Guangzhou Medical University, 63 Duobao Road, Liwan, Guangzhou, Guangdong 510150, P.R. China
E-mail: droctorycy1981@163.com

*Contributed equally

Key words: colorectal cancer, LINC02038, N6-methyladenosine, ceRNA, progression

Introduction

Colorectal cancer (CRC) is the third commonest type of cancer worldwide (1). Early clinical manifestations of CRC are nonspecific and it demonstrates significant tumor growth and early metastatic potential (2-4). Despite improvements in early diagnosis and systemic therapies, China and developed countries in Europe and the United States contribute to >50% of new CRC cases and associated mortalities globally (5). Consequently, there is an essential need to improve the understanding of the pathophysiology of CRC and provide CRC patients with novel treatment options.

Long noncoding RNAs (lncRNAs) are transcripts >200 nucleotides that do not encode proteins (6). lncRNAs are involved in a range of molecular mechanisms of cancer including miRNA sponging and RNA degradation (7-10). As biological techniques have advanced, numerous CRCrelated lncRNAs, including lncRNA GLCC1 (11), lncRNA ITGB8-AS1 (12) and H19 (13), have been linked to the progression of CRC via a range of mechanisms. The long intergenic noncoding RNA 2038 (LINC02038), which is located on chromosome 3q29, was found to be associated with the growth of CRC and serving as a crucial survival-related lncRNA (14). lncRNAs can function as competitive endogenous (ce)RNAs, which bind to microRNAs (miRNAs/miRs) in a competitive manner (15). Therefore, investigating the LINC02038 ceRNA pathways in CRC may uncover additional therapeutic options for the management of CRC. The location of the family with sequence similarity 172 member A (FAM172A) was discovered in chromosome 5q15. According to previous studies, FAM172A expression is highly tissue-specific and it inhibits the growth and metastasis of hepatocellular carcinoma (16). Overexpression of the PI3K/AKT signaling pathway has been linked to several types of cancer, including CRC and the PI3K/AKT signaling pathway is essential for the growth and metastasis of CRC (17).

In humans, the most prevalent form of RNA modification is N6-methyladenosine (m^{6}A) modification, which regulates RNA stability (18,19). A group of proteins regulate the cytoplasmic m^{6}A condition, termed 'writers' such as METTL3 and METTLI4 and 'readers' such as YTHDF2 and YTHDC2 and it has been shown that METTL3 was an important gene for CRC cell development (20).

In the present study, a correlation between the expression of LINC02038 and the clinical value of CRC patients was identified. Moreover, the functions of LINC02038 in cell growth, apoptosis and invasion from a functional analysis were ascertained. Further investigation confirmed that LINC02038 served as a sponge for miR-552-5p in CRC, enhancing its suppressive effect on FAM172A through the PI3K/Akt pathway. Furthermore, METTL3 exerted its function through weakening LINC02038 expression in an m^{6}A-YTHDF2-dependent manner. LINC02038 may provide novel CRC therapeutic approaches.

Materials and methods

Patients and tissue samples. A total of 68 CRC cases in total were collected from patients who received surgery at the First People's Hospital of Foshan between January 2018 and January 2020. Prior to resection, these individuals had not undergone chemotherapy or radiotherapy. All specimens were snap-frozen in liquid nitrogen and stored at -80˚C before use or fixed and paraffin-embedded. All patients provided informed consent and the Ethics Committee of the First People's Hospital of Foshan approved the present study (approval no. AF-SOP-18-1.6-2). The clinicopathological data of the patients are presented in Table I.

Cell culture and transfection. The human colorectal carcinoma cell lines used were LoVo, RKO, SW480, HCT116, DLD-1 and HT-29 cells and NCM460 normal colonic epithelial cell line were used as the control cells. All cells were obtained from the Cell Bank of Type Culture Collection of the Chinese Academy of Sciences. STR profiling was performed to verify the identity of the HT-29 cells. Cells were cultured in RPMI-1640 media supplemented with 10% FBS (Gibco; Thermo Fisher Scientific, Inc.) in a humidified incubator (95% humidity) supplied with 5% CO_2. Cells were routinely checked for Mycoplasma contamination. The overexpression vectors pcDNA3.1/Control (Vector) and pcDNA3.1/LINC02038 (LINC02038) were purchased from Shanghai GenePharma Co., Ltd.. Empty vector was used as the negative control (NC) for LINC02038 overexpression. A total of 3x10^5 cells/well were transfected with empty vector or pcDNA3.1-LINC02038 plasmids (1.5 μg/ml), a total of 30 pmol/l miR-552-5p mimics or mimic NC at room temperature for 48 h. The cells were collected for subsequent experiments at 48 h following transfection. miR-552-5p mimic and its negative control mimic for miR-552-5p, miR-552-5p inhibitor, were purchased from Shanghai GenePharma Co., Ltd.. The sequences were as follows: miR-552-5p mimics 5'-GUUUAACCUUUUGCCUGUUGG-3' and mimic NC 5'-UCACAACCUCCUAGAAAGAGUAGA-3'. Small interfering (si)RNAs against FAM172A (siFAM172A) and its scramble control siRNA were purchased from Shanghai GenePharma Co., Ltd. Vectors containing short hairpin (sh)RNAs targeting METTL3 (shMETTL3, i.e., shMETTL3-1 and shMETTL3-2) or its non-targeting shRNA sequence negative control (shNC METTL3), vectors containing short hairpin RNAs (shRNAs) targeting YTHDF2 (shYTHDF2, i.e., shYTHDF2-1 and shYTHDF2-2) or its non-targeting shRNA sequence negative control (shNC YTHDF2) were subcloned into Lv5 lentiviruses (Shanghai GenePharma Co., Ltd.) and were then transduced into the target cells. Transfection was performed using Lipofectamine® 3000 (Invitrogen; Thermo Fisher Scientific, Inc.). The efficacy of transfection was confirmed by reverse transcription-quantitative (RT-q) PCR.

Bioinformatics prediction. LINC02038, miR-552-5p and FAM172A levels were determined using The Cancer Genome Atlas (TCGA; https://cancergenome.nih.gov/) and the GEPIA (http://gepia.cancer-pku.cn) databases in CRC. The biological roles of LINC02038 were identified using the Kyoto Encyclopedia of Genes and Genomes (KEGG; https://www.genome.jp/kegg/). The miRcode (https://www.mircode.org/) and DIANA-LncBase Predicted v.2 (https://diana.e-ce.uth.gr/lncbasev2/home) online set of tools was used to predict the miRNAs targeted by LINC02038. TargetScan (http://www.targetscan.org/vert72/) and PicTar (https://pictar.mdcberlin.de) were used to predict mRNA target sites of miR-552-5p. SRAMP (http://www.cuilab.cn/sramp) was used to predict the possible m^{6}A modification locations of LINC02038.

RTqPCR. TRIzol® (Thermo Fisher Scientific, Inc.) was used to isolate total RNA from tissues and cells at a density of 3x10^6. A total of 500 ng RNA was used to synthesize cDNA by using a reverse transcriptase cDNA synthesis kit according to the manufacturer's protocol (Takara Bio, Inc.). The Hairpin-it MicroRNA and U6 snRNA Normalization RT-PCR Quantification kits were used to perform RT for miRNAs (Shanghai GenePharma, Co., Ltd.) according to the manufacturer's protocol. mRNA expression was determined using SYBR Premix ExTaq II (Takara Bio, Inc.) according to the manufacturer's protocol. The internal controls were GAPDH and U6. The thermocycling conditions were: Initial denaturation at 95˚C for 40 sec followed by 40 cycles of 95˚C for 10 sec, 20 sec at 60˚C and dissociation at 72˚C for 30 sec with a final extension step of 72˚C for 6 min. The $2^{-\Delta\Delta Cq}$ method was used to calculate the fold change (21). The primer sequences were: LINC02038 forward, 5'-ACCGTTTTTGATGGTGCTGC-3' and reverse, 5'-AAAACGCCTCTGTCGCAAAC-3'; METTL3 forward, 5'-AAGCTGCACTTCAGACGAAT-3' and reverse,5'-GGAATCACCTCCGACACTC-3'; YTHDF2 forward, 5'-AGCCCCACTTCCTACCAGATG-3' and reverse, 5'-TGAGAACTGTTATTTCCCCATGC-3'; GAPDH forward, 5'-AATGGGCAGCCGTTAGGAAA-3' and reverse, 5'-GCCCAATACGACCAAATCAGAG-3'; miR-552-5p forward, 5'-GTTTAACCTTTTGCCTGTTGG-3' and reverse, 5'-CGAACGCTTCACGAATTTG-3'; U6 forward, 5'-CTCGCTTCGGCAGCACA-3' and reverse, 5'-AACGCTTCACGAATTTGCGT-3'; and FAM172A forward, 5'-CAACGAGAAGCCGATGTA-3' and reverse, 5'-GATGTGTCTAATGGTTCTGAG-3'. All assays were repeated at least three times.

Cell Counting Kit8 (CCK8) assay. Cell vitality was determined using a CCK-8 assay (Dojindo Molecular Technologies, Inc.). LoVo and SW620 cells (1x10^3 cells/well) were plated

Table I. Relationship between LINC02038 expression and clinical characteristics in patients with colorectal cancer (n=68).

Parameter	Number of patients	LINC02038 expression		P-value
		Low	High	
Patients (n)	68	35	33	
Age (years)				0.902
≤60	32	17	15	
>60	36	18	18	
Sex				0.736
Female	26	13	13	
Male	42	22	20	
TNM stage				
I-II	29	10	19	0.011
III-IV	39	25	14	
Distant metastasis				0.024
Absent	57	27	30	
Present	11	8	3	
Differentiation				
Poorly or moderately	38	21	17	0.411
Well	30	14	16	
Tumor depth				
T1T2	32	12	20	0.022
T3T4	36	23	13	

into 96-well plates. After 24, 48, 72 or 96 h of transfection, each well was filled with RPMI-1640 containing 10% CCK-8 solution and cells were further incubated at 37˚C for 1 h. To assess the effectiveness of cell growth, a microplate reader was used to measure the absorption at 450 nm (Thermo Fisher Scientific, Inc.).

Flow cytometry. To fix cells, cells ($2x10^2$) were placed in 70% precooled ethanol overnight at 4˚C. To analyze cell cycle distribution, 400 μl propidium iodide (PI; Beyotime Institute of Biotechnology) was added to stain the cells, followed by incubation in the dark for 25 min at room temperature at 37˚C. A flow cytometer (FACScan; BD Biosciences) was used to determine the proportion of cells in each phase of the cell cycle. The data were analyzed using FlowJo 10 software (FlowJo LLC).

Annexin V-fluorescein isothiocyanate (FITC)/propidium iodide (PI) kits (Beyotime Institute of Biotechnology) were used to examine cell apoptosis. The cell pellet was washed with 4˚C precooled PBS followed by 1X binding buffer (centrifugation 300 x g, 5 min at 4˚C). A total of 250 μl 1X binding buffer was used to resuspend the cells and 5 μl Annexin V-FITC/PI staining was applied to the cells for 20 min at room temperature in the dark. Subsequently, 100 μl 1X binding buffer was added and flow cytometry was performed. The data (the percentage of early + late apoptotic cells) was examined using FlowJo 10 (FlowJo LLC).

Cell colony formation assay. A total of $1x10^3$ cells/well were incubated in 6-well plates using RPMI-1640 media containing 10% FBS at 37˚C and 5% CO_2 for 14 days. Subsequently, cells were fixed using methanol for 15 min and stained with 0.5% crystal violet at room temperature for 8 min. The colonies were counted using ImageJ software (version 1.5; National Institutes of Health).

Transwell assays. Cell migration and invasion were assessed using Transwell inserts pre-coated with Matrigel at 37˚C for 1 h or without Matrigel (Corning Inc.). To the upper chamber, $1x10^4$ cells suspended in 200 μl serum-free RPMI 1640 was added. To the lower chamber, 600 μl supplemented media was added. After 48 h of incubation, the cells that had migrated to the lower chamber were fixed using 4% paraformaldehyde for 30 min at room temperature and then stained with Giemsa for 15 min at room temperature. The number of cells in five randomly selected fields of view were imaged using a light microscope (Olympus Corporation). The number of cells that had migrated or invaded per field was determined using ImageJ (version 1.5; National Institutes of Health).

Fluorescence in situ hybridization (FISH) assays. GFP-labeled LINC02038 probes were supplied by Shanghai GenePharma Co., Ltd. A FISH kit (Shanghai GenePharma Co., Ltd.) was used to perform the hybridization. After being preserved with 4% paraformaldehyde at room temperature for 10 min, $2x10^4$ cells/well were permeabilized with 0.5% Triton X-100. and then washed three times with PBS. The cells were then supplemented with a prehybridization solution and blocked for 25 min at 37˚C. Cy3-labeled lncRNA FISH probes (Shanghai GenePharma Co., Ltd.) were used to detect LINC02038. The 2 μl and 15 μM probe mixture were added to the 100 μl

hybridization solution and this solution was added to cells for hybridization overnight at 37˚C. The nuclei were stained for fluorescence detection with DAPI at room temperature for 10 min and then mounted on glass slides in the dark setting. The fluorescence images were captured with an IX81 inverted fluorescence microscope with 5 fields of view being assessed per slide (Olympus Corporation).

Dual-luciferase reporter assay. In LoVo and SW620 cells, miR-552-5p interactions with LINC02038 or FAM172A were identified. Cells were co-transfected with vector, pmirGLO LINC02038 wild type (WT) or LINC02038 mutant (MUT), FAM172A WT or FAM172A MUT (Promega Corporation) as well as miR-552-5p mimic using Lipofectamine® 3000 (Invitrogen; Thermo Fisher Scientific, Inc.). Luciferase activity was determined after 48 h of transfection using the Dual-Luciferase Reporter assay system (Promega Corporation) according to the manufacturer's protocol.

RNA immunoprecipitation (RIP). To examine the relationship between miR-552-5p with LINC02038 or FAM172A in CRC cells, a Magna RIP RNA-Binding Protein Immunoprecipitation kit (cat: no. 17-700; Sigma, Millipore) and anti-argonaute 2 (Ago2) antibody (5 μg; cat. no. ab32381; Abcam) was used according to the manufacturer's protocol. Cells were centrifuged at 1,000 x g for 8 min at 4˚C and lysed in 600 μl RIP buffer (Millipore, Sigma). A total of 100 μl lysate was then treated with 5 μl normal IgG or 5 μl Ago2 antibody. The levels of LINC02038 or FAM172A and miR-552-5p enriched on beads were evaluated by RT-qPCR.

Western blotting. RIPA lysate solution (Invitrogen; Thermo Fisher Scientific, Inc.) was used to lyse the cells. A BCA assay (Beyotime Institute of Biotechnology) was used to determine the protein concentration. Total protein extracts (20 μg) was loaded on a 10% SDS-gel, resolved using SDS-PAGE, transferred to PVDF membranes (MilliporeSigma) and blocked for 1 h with 5% non-fat milk at room temperature. After blocking, membranes were incubated with one of the primary antibodies overnight at 4˚C. The antibodies used were: anti-FAM172A (cat. no. ab121364; 1:2,000; Abcam), anti-METTL3 (cat. no. ab195352; 1:1,000; Abcam), anti-YTHDF2 (cat. no. ab220163; 1:1,000; Abcam), anti-AKT (T308) (cat. no. ab38449; 1:1,000; Abcam), anti-AKT (cat. no. ab8805; 1:500; Abcam), anti-PI3K (cat. no. ab302958; 1:1,000; Abcam) and anti-GAPDH (cat. no. ab8245; 1:4,000; Abcam). After washing with PBS, the membranes were probed for 1 h at room temperature and incubated with goat anti-rabbit IgG secondary antibody (cat. no. ab97080; 1:5,000; Abcam) and goat anti-mouse IgG secondary antibody (cat. no. ab97040; 1:5,000; Abcam). Pierce ECL reagent (Pierce; Thermo Fisher Scientific, Inc.) was used to observe the protein bands and ImagePro Plus software version 6.0 (Media Cybernetics, Inc.) was used for densitometry analysis.

In vivo experiments. A total of 18 male BALB/c nude mice (age, 4 weeks; weight, 14-18 g) were purchased from Southern Medical University Experimental Animal Centre and were kept in the pathogen-free-grade research center at 28˚C with 50% humidity, with a 12 h light/dark cycle and *ad libitum* access to food and water. The Institutional Animal Care and Use Committee of the Southern Medical University approved the animal experiments (approval no. 2032101). A total of 2x10^4 LoVo cells stably overexpressing LINC02038 or LINC02038 or pcDNA3.1/Control (Vector) were subcutaneously injected in the dorsal flank of mice. The weight and growth of the tumor were assessed every 5 days. The volume of the tumor was calculated as follows: Volume (mm^3)=(width^2 x length)/2. At 3 weeks following inoculation, cervical dislocation was used to euthanize the mice after isoflurane inhalation (5% for 5 min). Finally, tumor tissues were used for immunohistochemistry (IHC) analysis. The National Institutes of Health Guide for the Care and Use of Laboratory Animals was followed when conducting the study. The maximum tumor volume observed was 534 mm^3 and the maximum tumor diameter was 17 mm.

Immunohistochemistry (IHC). After being fixed with 4% paraformaldehyde at 4˚C for 24 h and then dehydrated in ethanol from low to high concentration, permeabilized using xylene and embedded in paraffin, tumor tissues were embedded in paraffin and sectioned at 4 μm. For inhibiting endogenous peroxidases, dewaxed portions were cleared with xylene and were then rehydrated in an descending ethanol gradient at room temperature for 15 min prior to incubation with 3% H_2O_2 for 10 min. For antigen retrieval, samples were placed in citrate solution (pH 6.0) at 95˚C for 15 min. The plates were treated with primary antibodies against Ki-67 (cat. no. ab15580; 1:400; Abcam) and FAM172A (cat. no. ab121364; 1:300; Abcam) overnight at 4˚C. Subsequently, the sections were treated with an HRP-conjugated secondary antibody for 60 min at 37˚C prior to incubation with diaminobenzidine (DAB). The slices were counterstained with hematoxylin for 3 min at room temperature. Images were captured using a light microscope (Olympus Corporation).

m^{6}A quantification. Total RNA was quantified and purified using a Dynabeads mRNA Purification kit (Thermo Fisher Scientific, Inc.). The m^{6}A quantification of mRNA was measured using the EpiQuik m^{6}A Methylation Quantification kit according to the manufacturer's protocol (Colorimetric; EpigenTek).

m^{6}A-RNA immunoprecipitation-qPCR (MeRIP-qPCR). MeRIP-qPCR was performed as described previously (22). Briefly, mRNA was isolated, purified and fragmented chemically using Ambion fragmentation reagent (Thermo Fisher Scientific, Inc.) into 100-nt pieces prior to being incubated with 15 μl ChIP Protein Magnetic Beads (MilliporeSigma) conjugated to 2 μg of anti-m^{6}A polyclonal antibody (cat. no. ab208577; Abcam) or mouse control IgG in 1X IPP buffer, 250 ng mRNA fragments were denatured at 65˚C for 5 min. Subsequently, incubation of mRNA with m^{6}A-bound beads in IPP buffer at 4˚C with constant rotation for 2 h was washed with different types of buffers in turn. As the final step, the RNA was eluted and purified using Qiagen RNeasy columns (Qiagen GmbH) in 200 μl RNase-free water. The abundance of RNA was assessed using qPCR as described above according to the manufacturer's protocol. The experiments were repeated three times.

RNA stability. A total of $1x10^3$ cells/well were incubated with 10 g/ml actinomycin D overnight in a CO_2-free humidified incubator. Total RNA was isolated and quantified after 0, 1, 2, 4, or 8 h of actinomycin D treatment, using RT-qPCR as described above according to the manufacturer's protocol. The experiments were repeated three times.

Statistical analysis. Analysis was performed using GraphPad Prism version 9.0 (Dotmatics). Data are presented as the mean ± standard deviation. A Student's t-test or a one-way ANOVA followed by Tukey's test was used to evaluate differences between groups. The association between LINC02038 transcript and clinicopathological characteristics were investigated using a Fisher's exact test or a χ^2 test. Using linear regression analysis, the association between two genes was analyzed. Kaplan-Meier analysis with log-rank test was used to assess the overall survival rate. $P<0.05$ was considered to indicate a statistically significant difference.

Results

LINC02038 is downregulated in CRC. The expression patterns of lncRNAs in CRC specimens were obtained from the TCGA and GTEx databases. LINC02038 was one of the most downregulated lncRNAs with a fold change (FC) of ≥5 and a P-value of <0.05 (Fig. 1A), indicating that it could be a tumor suppressor lncRNA as well as a therapeutic target and prognostic biomarker in CRC. A total of 1,263 differentially expressed lncRNAs were identified (Fig. 1B). The expression of LINC02038 in various tumor types was assessed and found to be lower than in normal samples when analyzed using the TCGA and GTEx datasets (Fig. 1C). Additionally, GEO databases were examined using the R tool to determine LINC02038 expression. The results showed that LINC02038 expression was typically lower in tumor specimens compared to normal tissues (Fig. 1D and E). Furthermore, LINC02038 expression was positively associated with higher overall survival (OS) according to the GEPIA database (Fig. 1F). KEGG analysis showed that LINC02038 was closely related to the PI3K/Akt signaling pathway (Fig. 1G). Subsequently, the potential clinical relevance of LINC02038 was investigated. The results showed positive associations between low LINC02038 expression and high invasion, distant metastasis and higher TNM stage (Table I).

LINC02038 regulates apoptosis and proliferation, migration and invasion of CRC cells. To further verify the potential of LINC02038, its expression was analyzed in colorectal cancer (CRC) specimens and cell lines (HT-29, LoVo, SW620, SW480, HCT116 and DLD-1) using RT-qPCR. RT-qPCR analysis showed that LINC02038 was considerably downregulated in CRC tissues relative to adjacent normal colorectal tissues (n=68 pairs; Fig. 2A). In comparison with normal colorectal epithelial cells (NCM460), the expression of LINC02038 was greatly decreased in various CRC cell lines (Fig. 2B,C). To determine the role of LINC02038 in CRC progression, LoVo and SW620 cells were transfected with pcDNA3.1-LINC02038. RT-qPCR results showed that transfection with the LINC02038 vector dramatically increased LINC02038 expression (Fig. 2D). CCK-8 assay indicated that the LINC02038-overexpressed LoVo and SW620 cells proliferated a reduced amount than the control cells (Fig. 2E). Colony formation assay results demonstrated that the upregulation of LINC02038 inhibited the growth of LoVo and SW620 cells (Fig. 2G). Notably, an increasing number of CRC cells in the G_1/G_0 phase and a decrease in the number in the S phase were detected in response to LINC02038 overexpression compared to control groups using flow cytometry (Fig. 2F). Furthermore, flow cytometry results showed that overexpression of LINC02038 increased the percentage of apoptotic cells compared to the empty vector group (Fig. 2H). Cell motility was measured using Transwell assays and the results showed that overexpression of LINC02038 hindered migration and invasion capacities of LoVo and SW620 cells (Fig. 2I and J).

LINC02038 acts as a sponge for miR-552-5p in CRC. As the role of lncRNAs can be determined by their subcellular location, the subcellular localization of LINC02038 was observed using FISH. The results showed that LINC02038 was predominantly localized in the cytoplasm (Fig. 3A). Additionally, the binding sites between LINC02038 and miR-552-5p were predicted using miRcode and LncBase Predicted v.2 (Fig. 3B). Furthermore, the relationship between LINC02038 and miR-552-5p was investigated in data on patients with primary colon adenocarcinoma (COAD) obtained from TCGA. The results showed that LINC02038 expression was found to be inversely associated with miR-552-5p expression in CRC (Fig. 3C). Using the TCGA-COAD dataset, it was demonstrated that miR-552-5p expression was significantly increased in CRC tissues when compared with the adjacent normal tissues (Fig. 3D). This result was confirmed using RT-qPCR analysis which showed that miR-552-5p expression was higher compared with adjacent tissues (Fig. 3E) and cells (Fig. 3F) than that of the adjacent non-tumor tissues and NCM460 cells. Additionally, LINC02038 overexpression substantially reduced miR-552-5p levels of CRC cells based on the results of RT-qPCR (Fig. 3G).

To further confirm the interaction of LINC02038 with miR-552-5p, dual-luciferase reporter plasmids with WT or MUT putative binding sites of LINC02038 transcripts were constructed. The luciferase activity was substantially decreased in cells co-transfected with LINC02038-WT and miR-552-5p mimics. However, no statistical changes in luciferase activity were observed when cells were co-transfected with LINC02038-MUT and miR-552-5p mimics (Fig. 3H). In the cell cytoplasm, AGO2, together with GW182 have a role in executing miRNA-mediated repression. While miRNAs guide AGO2 to target mRNAs, a direct interaction between AGO2 and GW182 proteins is required for the assembly of ribonucleoprotein complexes, named RNA-induced silencing complexes (RISCs) and the recruitment of additional factors involved in gene silencing, which is ultimately achieved through the degradation of target mRNAs or translational repression (23). RNA-binding protein immunoprecipitation can systematically identify RISC-bound miRNAs and their target mRNA sequences in mammalian cells (24). LINC02038 was enriched when the Ago2 antibody was used in RIP studies in SW620 and LoVo cells (Fig. 3I), demonstrating that LINC02038 directly binds to miR-552-5p. Additionally, there was an inverse correlation between LINC02038 expression and OS in the TCGA-COAD dataset (Fig. 3J).

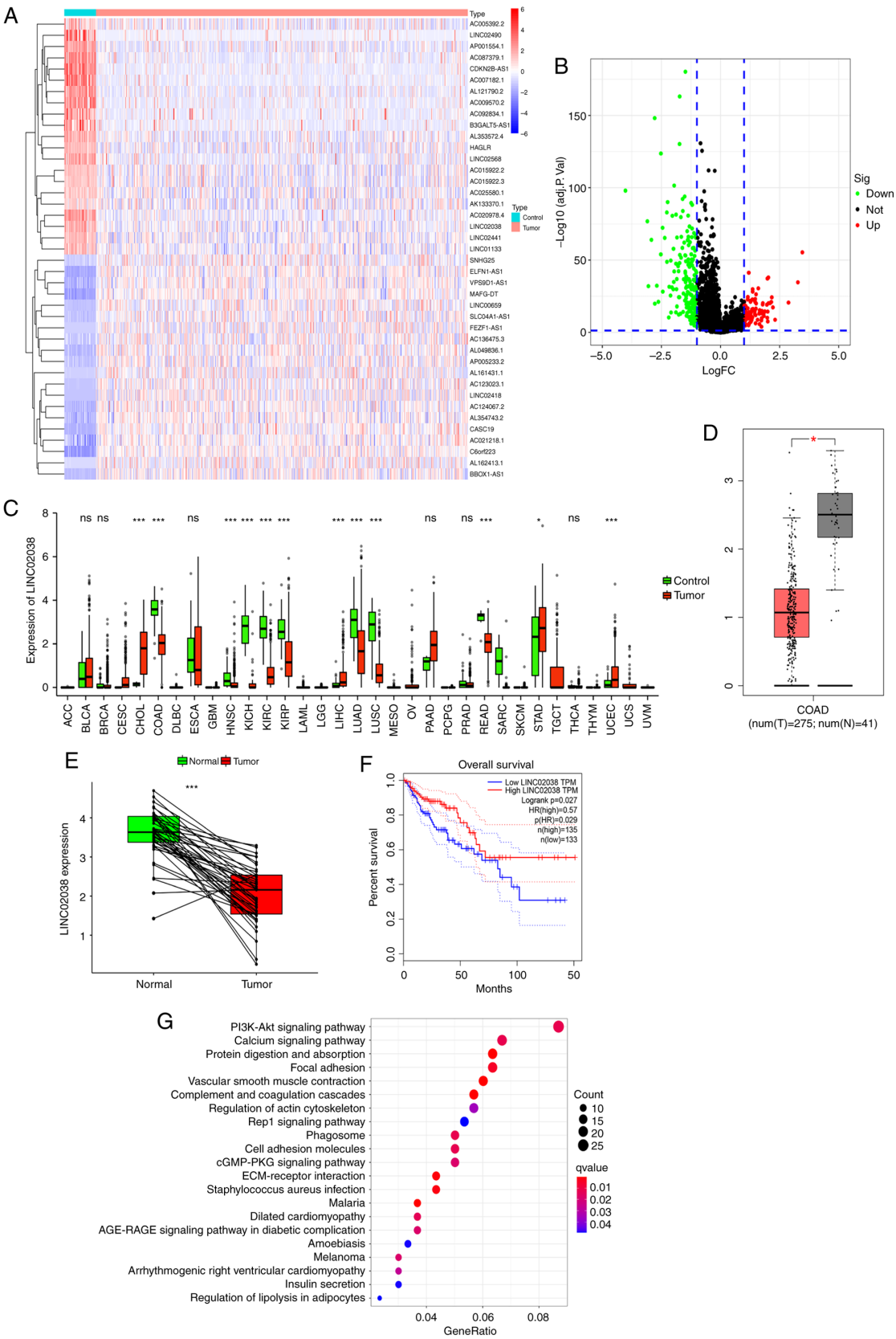

Figure 1. LINC02038 is downregulated in CRC. (A) Heatmap of lncRNAs. lncRNAs with an FC ≥5 and P<0.05 were considered down- or upregulated. Downregulation is represented by a blue scale, while upregulation is represented by a red scale. (B) lncRNA volcano diagram of CRC vs. non-tumorous tissues. Upregulated genes are indicated in red and downregulated genes are indicated in green (defined by FC ≥1 and P<0.05). Genes in black were differentially expressed by FC <1. (C) Expression of LINC02038 based on pan-cancer analysis utilizing the TCGA and GTEx databases. LINC02038 expression was lower in COAD tissues than in normal colorectal tissues. (D and E) The expression of LINC02038 in CRC and normal colorectal tissues based on data obtained from GTEx and TCGA datasets. (F) The relationship between the LINC02038 and OS in the obtained datasets. (G) Bubble plots showing the top 21 dysregulated KEGG pathways in terms of genes associated with LINC02038 in CRC. *P<0.05, ***P<0.001. CRC, colorectal cancer; lncRNA, long non-coding RNA; TCGA, The Cancer Genome Atlas; GTEx, Genotype-Tissue Expression project; KEGG, Kyoto Encyclopedia of Genes and Genomes; COAD, colon adenocarcinoma; OS, overall survival; ns, no significance.

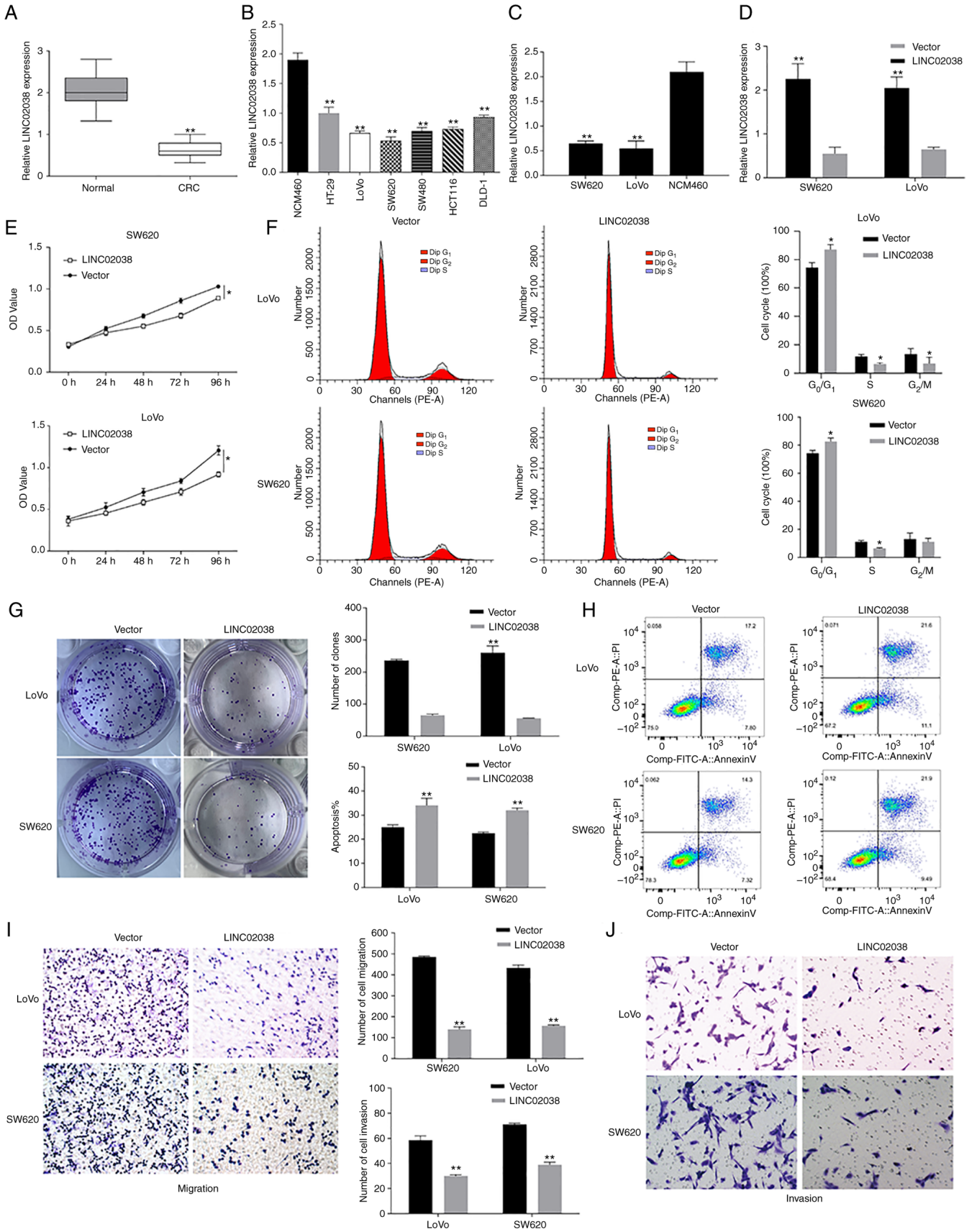

Figure 2. LINC02038 suppresses CRC cell growth, motility and invasion while inducing apoptosis. (A) LINC02038 expression in 68 paired CRC and normal colorectal tissue. (B and C) LINC02038 expression in several different CRC cell lines. (D) LINC02038 was successfully overexpressed in CRC cells transfected with pcDNA3.1-LINC02038. (E) CCK-8 assay results showed the proliferative effects of LINC02038 overexpression on CRC cells. (F) Overexpression of LINC02038 affected CRC cell cycle regulation. (G) CRC proliferation was detected using colony formation assays following LINC02038 overexpression. (H) Overexpression of LINC02038 promoted apoptosis in a fraction of the cells as measured by flow cytometry. Transwell assays showing CRC (I) migration and (J) invasion following LINC02038 overexpression. Magnification, x200. *P<0.05, **P<0.01 vs. normal tissues, NCM460, or empty vector; CRC, colorectal cancer.

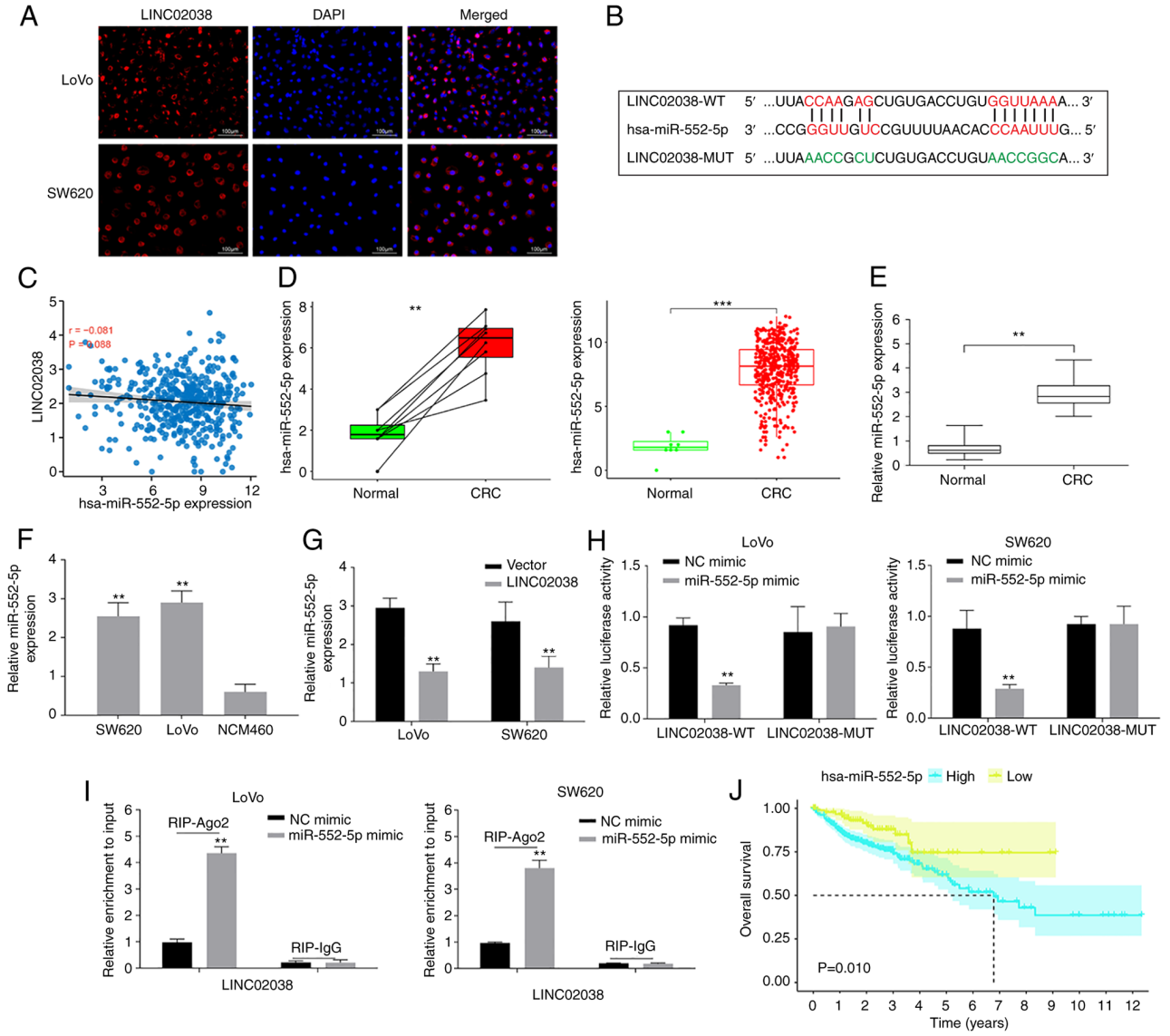

Figure 3. LINC02038 sponges miR-552-5p in the CRC cells. (A) LINC08038 localized to the cytoplasm (red) and nucleus (blue) in LoVo and SW620 cells using FISH test. (B) The predicted binding site between LINC02038 and miR-552-5p. (C) Using data obtained from TCGA-COAD dataset, it was shown there was a negative association between LINC02038 and miR-552-5p expression in CRC tissues. (D) TCGA-COAD database analysis confirmed that miR-552-5p expression was higher in CRC tissues than in matched and unpaired normal tissues. (E) RT-qPCR analysis of miR-552-5p expression in CRC and normal tissues. (F) RT-qPCR detection of miR-552-5p expression in CRC cells. (G) miR-552-5p expression in LoVo and SW620 cells transfected with LINC02038 overexpression or an empty vector was determined using RT-qPCR. (H) The relative luciferase activity in LoVo and SW620 cells co-transfected with LINC02038 WT or MUT and miR-552-5p mimics. (I) RIP assays were used to examine LINC02038 enrichment in LoVo and SW620 cells co-transfected with LINC0203 and miR-552-5p mimic. (J) The relationship between miR-552-5p and overall survival in CRC patients in TCGA-COAD dataset. **P<0.01, ***P<0.001. miR, microRNA; CRC, colorectal cancer; FISH, Fluorescence *in situ* hybridization; TCGA, The Cancer Genome Atlas; COAD, colon adenocarcinoma; RT-qPCR, reverse transcription quantitative PCR; MUT, mutant; WT, wild-type; Ago2, argonaute 2; RIP, RNA immunoprecipitation.

LINC02038 inhibits CRC progression by targeting miR-552-5p. To study the effect of LINC02038 on miR-552-5p, miR-552-5p mimic and inhibitor and LINC02038 overexpression vector were transfected into SW620 and LoVo cells. The results indicated that overexpression of LINC02038 significantly reduced miR-552-5p expression levels (Fig. 4A). It was shown that miR-552-5p promoted proliferation, migration and invasiveness as well as reduced apoptosis. To evaluate whether miR-552-5p regulated the molecular functions of LINC02038 in SW620 and LoVo cells, rescue experiments were conducted. The results showed that transfection of LINC02038 overexpression vector reversed the effect of miR-552-5p mimics on growth (Fig. 4B and C), migration (Fig. 4F) and invasiveness (Fig. 4G) and the inhibition of cell apoptosis (Fig. 4E). Cell cycle analysis showed that the proportion of SW620 and LoVo cells in the S phase of the cycle was increased after miR-552-5p mimic transfection, whereas LINC02038 led to an arrest of cell in the G_1 phase (Fig. 4D).

FAM172A is a direct target gene of miR-552-5p. FAM172A binding to miR-552-5p was identified using TargetScan and PicTar (Fig. 5A). Thus, FAM172A expression was studied in TCGA datasets. FAM172A in CRC tissues was lower than in the non-tumor tissues (Fig. 5B and C). Furthermore, RT-qPCR and western blot analyses indicated that FAM172A

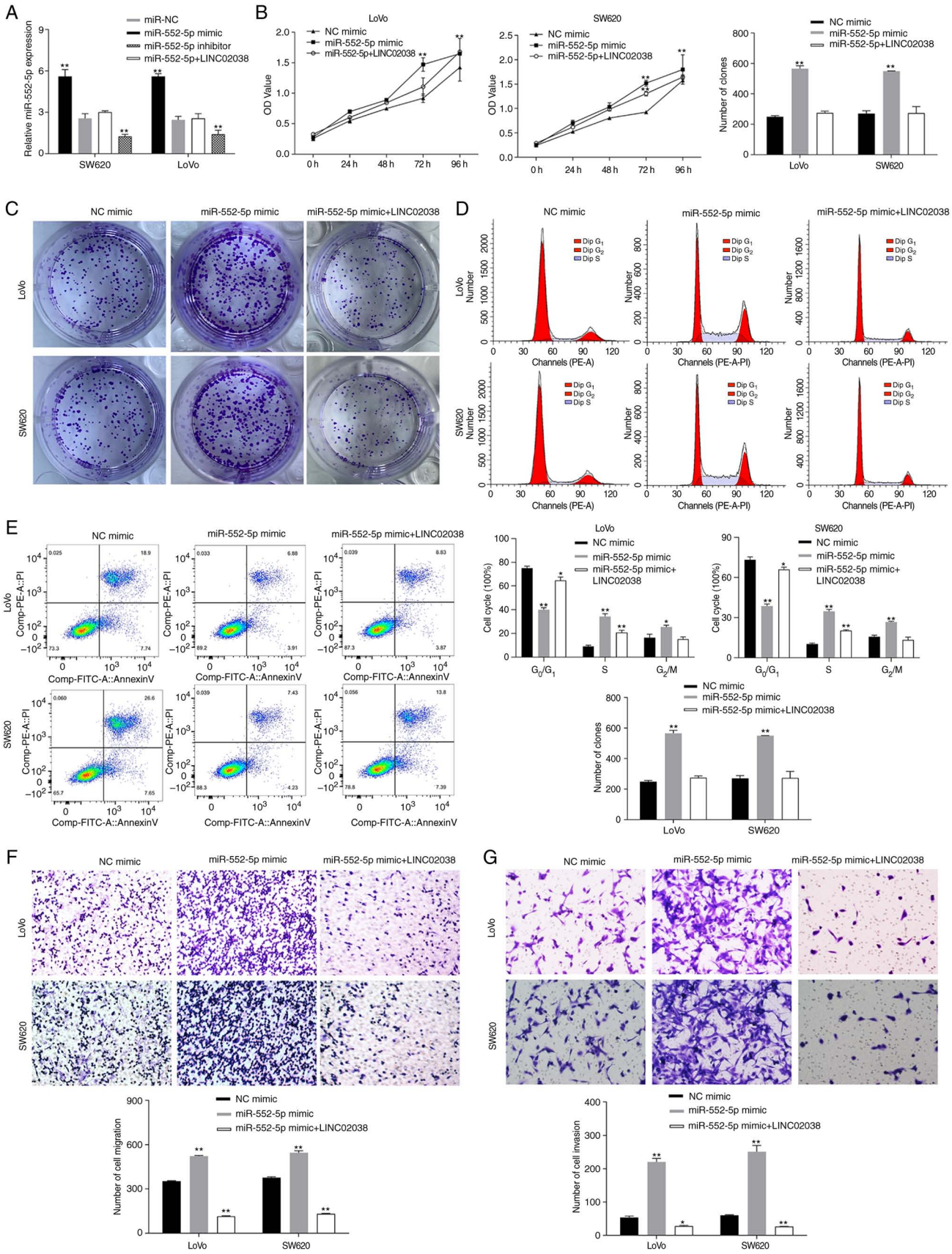

Figure 4. LINC02038 exerts its function by inhibiting miR-552-5p in CRC cells. (A) miR-552-5p expression was determined using RT-qPCR after transfection with miR-552-5p mimic, LINC02038 overexpression + miR-552-5p mimic or the control. (B) CCK-8 and (C) colony formation assays were used to assess the proliferation of transfected cells. (D and E) Flow cytometry was used to identify the cell cycle distribution and apoptosis of SW620 and LoVo cells transfected with miR-552-5p mimic, LINC02038 overexpression + miR-552-5p mimic or the control. LINC02038 overexpression resulted in G_1 phase cell cycle arrest and increased rates of apoptosis and partially reversed the effects of miR-552-5p mimic transfection in CRC cells. (F) Migration and (G) invasion rates were determined using Transwell assays in CRC cells co-transfected with LINC02038 overexpression vector and miR-552-5p mimics as well as the corresponding controls. *P<0.05, **P<0.01 vs. NC mimic; miR, microRNA; CRC, colorectal cancer; RT-qPCR, reverse transcription quantitative PCR; NC, negative control.

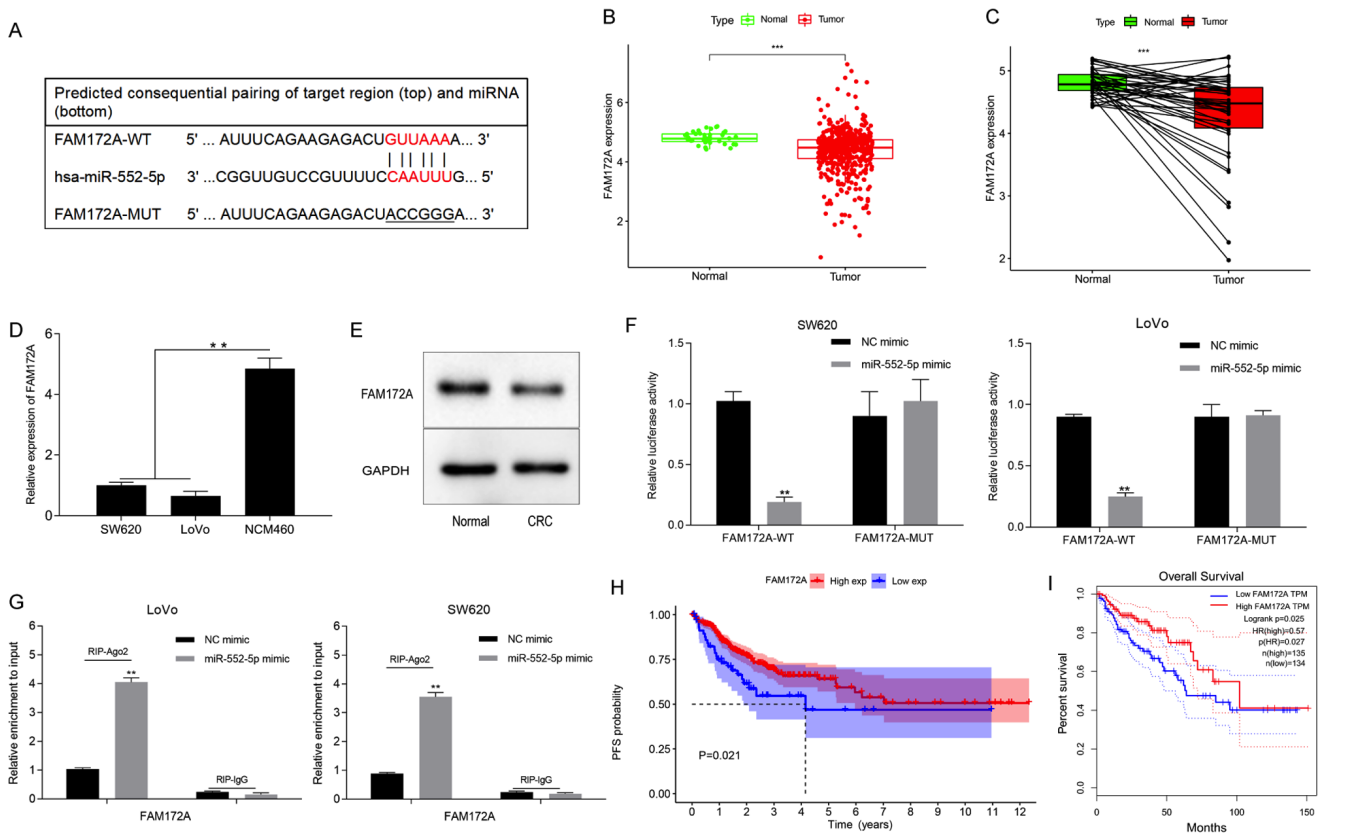

Figure 5. miR-552-5p targets and regulates FAM172A. (A) Bioinformatics analysis revealed that miR-552-5p directly targets the 3'-UTR of FAM172A. (B and C) Differential FAM172A expression in CRC and normal tissues. FAM172A expression in (D) several CRC cell lines was determined using RT-qPCR and (E) in CRC tissues by western blotting. (F) The luciferase activity of the reporter including miR-552-5p mimic and FAM172A WT or MUT was evaluated. (G) RIP assay analysis showed FAM172A or miR-552-5p expression pulled down from the lysates of SW620 and LoVo cells with the anti-Ago2 antibody. Data obtained from TCGA was utilized to investigate the association between FAM172A expression and the (H) PFS and (I) overall survival in CRC patients. Data are presented as the mean ± SD of three repeats. **P<0.01, ***P<0.001. miR, microRNA; UTR, untranslated region; CRC, colorectal cancer; RT-qPCR, reverse transcription quantitative PCR; WT, wild-type; MUT, mutant; RIP, RNA immunoprecipitation; TCGA, The Cancer Genome Atlas; PFS, progression free survival; NC, negative control.

was downregulated compared to the normal colorectal cell line (Fig. 5D) and tissues (Fig. 5E). In addition, luciferase reporter assay showed a substantial decrease in luciferase activity following co-transfection with the FAM172A-WT and miR-552-5p mimics, while there was no substantial change in cells co-transfected with FAM172A-MUT and miR-552-5p mimics (Fig. 5F). RIP studies were performed using the SW620 and LoVo cells. The results revealed that FAM172A co-precipitated miR-552-5p (Fig. 5G). In addition, the GEPIA database indicated that low FAM172A expression was associated with a lower progression-free survival and OS (Fig. 5H and I).

FAM172A silencing counteracts the inhibitory effects of LINC02038 overexpression in CRC. To ascertain whether the biological functions of LINC02038 would change if FAM172A was silenced, a FAM172A knockdown vector was transfected into CRC cells. The findings revealed that FAM172A expression was reduced in SW620 and LoVo cells transfected with siFAM172A (Fig. 6A). Additionally, the protein and mRNA expression levels of FAM172A were significantly suppressed in the si-FAM172A group, but these effects were reversed after co-transfection of LINC02038 overexpression and si-FAM172A (Fig. 6B and C). Downregulation of FAM172A increased proliferation (Fig. 6D and E), migration and invasiveness (Fig. 6H and I) and inhibited apoptosis (Fig. 6G) of the SW620 and LoVo cells, but these effects were abolished by overexpression of LINC02038. Cell cycle distribution analysis revealed that in SW620 and LoVo cells there was an increased proportion of cells that had accumulated in the S phase of the cell cycle following siFAM172A transfection. However, following co-transfection of siFAM172A and LINC02038 overexpression in the CRC cells, G_1 phase arrest was observed (Fig. 6F). Furthermore, p-Akt and PI3K protein expression levels were increased after transfection of siFAM172A, whereas this was reversed in the CRC cells co-transfected with LINC02038 overexpression and siFAM172A (Fig. 6J).

Effect of LINC02038 on tumor growth in vivo. In a xenograft model of tumor growth, LoVo cells transfected with LINC02038 overexpression or an NC vector were subcutaneously implanted into nude mice. Mice were euthanized after 4 weeks of injection and tumors were retrieved. Compared to the control group, the tumor volume and weight were lower in the LINC02038 overexpression group (Fig. 7A-C). Moreover, immunohistochemical staining of tumor specimens showed that Ki-67 expression was significantly downregulated

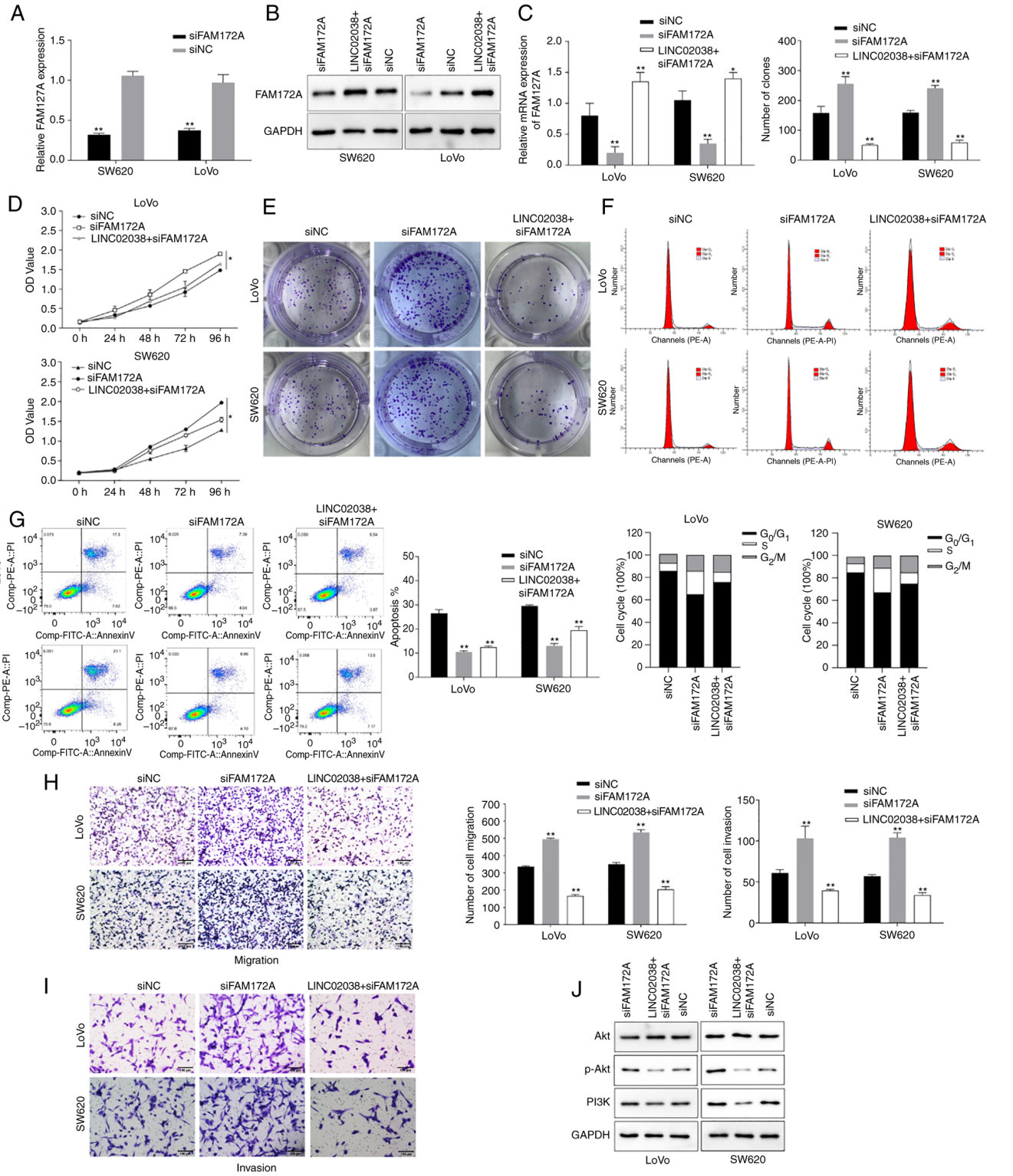

Figure 6. LINC02038 inhibits CRC progression by regulating FAM172A. (A) The knockdown efficiency of siRNAs targeting FAM172A was validated using RT-qPCR. (B) FAM172A expression was examined using western blotting in the FAM172A knockdown cells and/or LINC02038 overexpressing cells. (C) FAM172A mRNA levels are shown in SW620 and LoVo cells co-transfected with siFAM172A and LINC02038 overexpression vector. (D and E) CCK-8 and colony formation assays were used to evaluate cell viability. (F) Flow cytometry was used to examine the cell cycle distribution. (G) Apoptosis was detected in SW620 and LoVo cells using Annexin V/PI double-staining by fluorescence activated cell sorting. Transwell assays were used to evaluate (H) migration and (I) invasion of SW620 and LoVo cells. Scale bars, 100 μm. (J) The protein expression levels of AKT, p-AKT and PI3K were analyzed by western blotting in SW620 and LoVo cells. Data are presented as the mean ± SD of three repeats. *P<0.05, **P<0.01. CRC, colorectal cancer; siRNA, small interfering RNA; RT-qPCR, reverse transcription quantitative PCR; p-, phosphorylated.

but FAM172A expression was notably upregulated in the LINC02038 overexpression group compared with the control group (Fig. 7D). *In vivo*, LINC02038 effectively inhibited tumor growth.

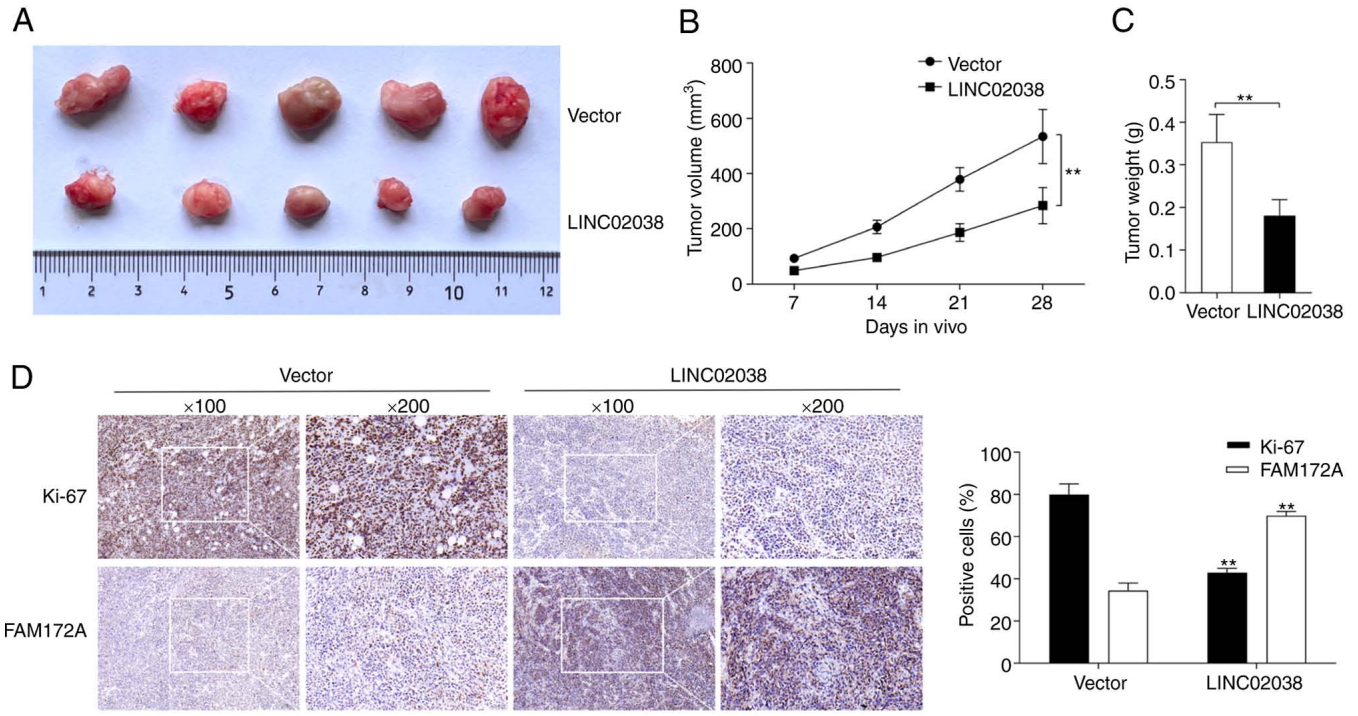

Figure 7: *In vivo*, LINC02038 inhibits CRC tumorigenesis. (A) Images of the CRC tissues following subcutaneous injection of LoVo cells with LINC02038 overexpression or pcDNA3.1/Control empty vector. The (B) volume and (C) weight of xenograft tumors were measured. (D) Representative images of IHC-stained CRC tissues. Magnification, x100 and x200. Data are presented as the mean ± SD of three repeats. **P<0.01. CRC, colorectal cancer; IHC, immunohistochemistry.

METTL3-mediated m^{6}A modification is associated with LINC02038 downregulation through a YTHDF2-dependent mechanism in CRC. To further verify the regulatory mode of LINC02038, SRAMP (http://www.cuilab.cn/sramp/) analysis was utilized to predict m^{6}A modification sites. It was discovered that LINC02038 contained an abundance of m^{6}A modification sites, indicating that it was particularly susceptible to m^{6}A methylation (Fig. 8A). Moreover, the MeRIP results revealed that LINC02038 has a number of fragments modified by RNA methylation (Fig. 8B). In addition, METTL3 was expression was downregulated in LoVo and SW620 cells using two shRNAs targeting METTL3 (shMETTL3-1 and shMETTL3-2), which markedly attenuated the mRNA and protein expression of levels of METTL3 (Fig. 8C). According to the bioinformatics analysis using TCGA, METTL3 expression was inversely correlated with LINC02038 expression (Fig. 8D). Additionally, LINC02038 expression was significantly upregulated in CRC cells transfected with shMETTL3 (Fig. 8E). MeRIP-qPCR results suggested that the m^{6}A abundance in the LINC02038 mRNA was notably reduced following METTL3 knockdown (Fig. 8F). Subsequently, the findings of the RIP assays revealed that METTL3 and YTHDF2 could enrich LINC02038 (Fig. 8G). RT-qPCR results demonstrated that YTHDF2 was successfully knocked down using two shRNA targeting YTHDF2 (shYTHDF2-1 and shYTHDF2-2) in LoVo and SW620 cells, which markedly weakened YTHDF2 mRNA and protein levels (Fig. 8H); LINC02038 expression was upregulated in LoVo and SW620 cells transfected with shYTHDF2 (Fig. 8I) and knockdown of YTHDF2 reduced the degradation of LINC02038 (Fig. 8J).

Discussion

The aim of the present study was to determine the clinical importance of LINC02038 and its role in the progression of CRC, as well as to explore its potential molecular mechanisms. TCGA and GEO datasets were analyzed and the results were validated in CRC samples. It was discovered that LINC02038 played a significant role in CRC. The findings showed that LINC02038 was notably downregulated in CRC tissues and cell lines. Additionally, it was found that low expression of LINC02038 was associated with poor prognosis in CRC, suggesting that it could have been a potential prognostic target for this disease.

The present study examined whether LINC02038 was a unique tumor-suppressing lncRNA that regulated the growth and aggressiveness of CRC. The results of gain-of-function assays showed that LINC02038 suppressed CRC cell proliferation, migration and invasiveness while promoting apoptosis. *In vivo* experiments revealed that LINC02038 inhibited CRC tumor growth, demonstrating its tumor suppressor function in CRC. Studies have shown the importance of lncRNAs in carcinogenesis and antitumor behavior, with dysregulation of lncRNAs being closely associated with tumor formation (25,26). CRC-specific diagnosis, prognosis and therapies may target specific lncRNAs (27). Potentially viable treatments for advanced CRC may involve regulating lncRNAs with specific expression patterns. Therefore, understanding the function and regulation processes of lncRNAs is critical. LINC02038 is a 2,434 nucleotide-long intergenic non-protein coding RNA involved in CRC prognosis (14). However, its ability to regulate cellular processes through interactions

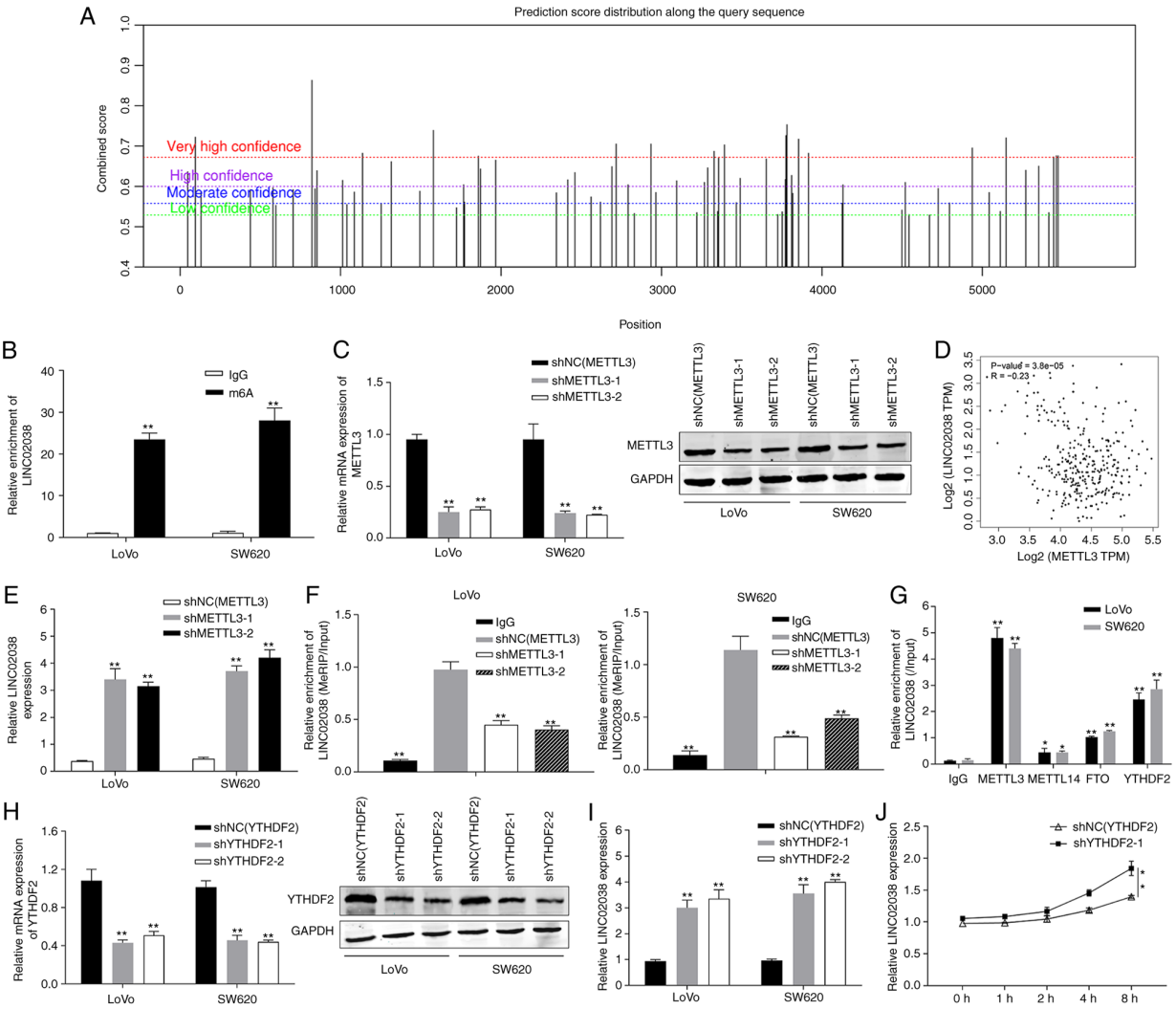

Figure 8. METTL3 knockdown reduces the stability of LINC02038 via an m^{6}A-YTHDF2-dependent mechanism. (A) SRAMP was used to predict the possible m^{6}A modification locations of LINC02038. (B) The enrichment of m^{6}A-modified LINC02038 was measured using a MeRIP-qPCR assay. (C) Using RT-qPCR and western blotting, METTL3 expression was determined in CRC cells following METTL3 knockdown. (D) Correlation analysis of METTL3 and LINC02038 mRNA on data obtained from TCGA. (E) LINC02038 expression in METTL3-deficient LoVo and SW620 cells was detected using RT-qPCR. (F) shMETTL3-mediated LINC02038 m^{6}A modifications were demonstrated in LoVo and SW620 cells. (G) The interaction between METTL3, METTL14, FTO and YTHDF2. (H) YTHDF2 expression of LoVo and SW620 cells transfected with shYTHDF2 were detected using RT-qPCR and western blotting. (I) LINC02038 expression was determined using RT-qPCR in YTHDF2-deficient LoVo and SW620 cells. (J) The expression of LINC02038 was detected following treatment with Actinomycin D (5 mg/ml) in SW620 cells using RT-qPCR at the indicated time points. Data are presented as the mean ± SD of three repeats. *P<0.05, **P<0.01. m^{6}A, N6-methyladenosine; MeRIP, methylated RNA immunoprecipitation; qPCR, quantitative PCR; RT-qPCR, reverse transcription qPCR; TCGA, The Cancer Genome Atlas; shRNA, short hairpin RNA.

with other cellular components remains to be elucidated. To understand the function of an lncRNA, knowledge about its subcellular distribution within the cell is required (28). The present study found that LINC02038 was mainly located in the cytoplasm of CRC cells. Theoretically, LINC02038 may affect fundamental biological processes such as methylation and post-transcriptional regulation.

The majority of cytoplasmic lncRNAs act as ceRNAs to modulate downstream mRNA expression by competitively suppressing miRNA expression through the presence of miRNA response elements (29). For example, LINC01133 can elicit biological behaviors as a ceRNA by interacting with the target sequence of miR-106a-3p, thereby expanding the roles of APC mRNA targets (30). Xu *et al* (31) reported that lncRNA SNHG6 was elevated in colorectal cancer (CRC) and enhanced the invasiveness of CRC cells by sponging miR-26a/b and miR-214. Dual-luciferase reporter and RIP assays indicated that LINC02038 absorbed miR-552-5p. Previous studies have shown that miR-552-5p is an oncogene in various types of human cancer and promotes cell proliferation and metastasis (32,33). Mechanistically, LINC02038 functions as a ceRNA for miR-552-5p, inhibiting CRC cell proliferation, migration and invasion while promoting apoptosis. These findings may offer novel therapeutic strategies for CRC. The miRNA target gene is essential for the function of lncRNAs as ceRNAs. Using TargetScan and PicTar online databases, FAM172A was identified as a potential target of miR-552-5p. Luciferase reporter and RIP assay results showed that FAM172A was a downstream target gene of miR-552-5p. Previous studies have indicated that FAM172A may play an important role in inhibiting human cancer cell growth by regulating different signaling pathways. For

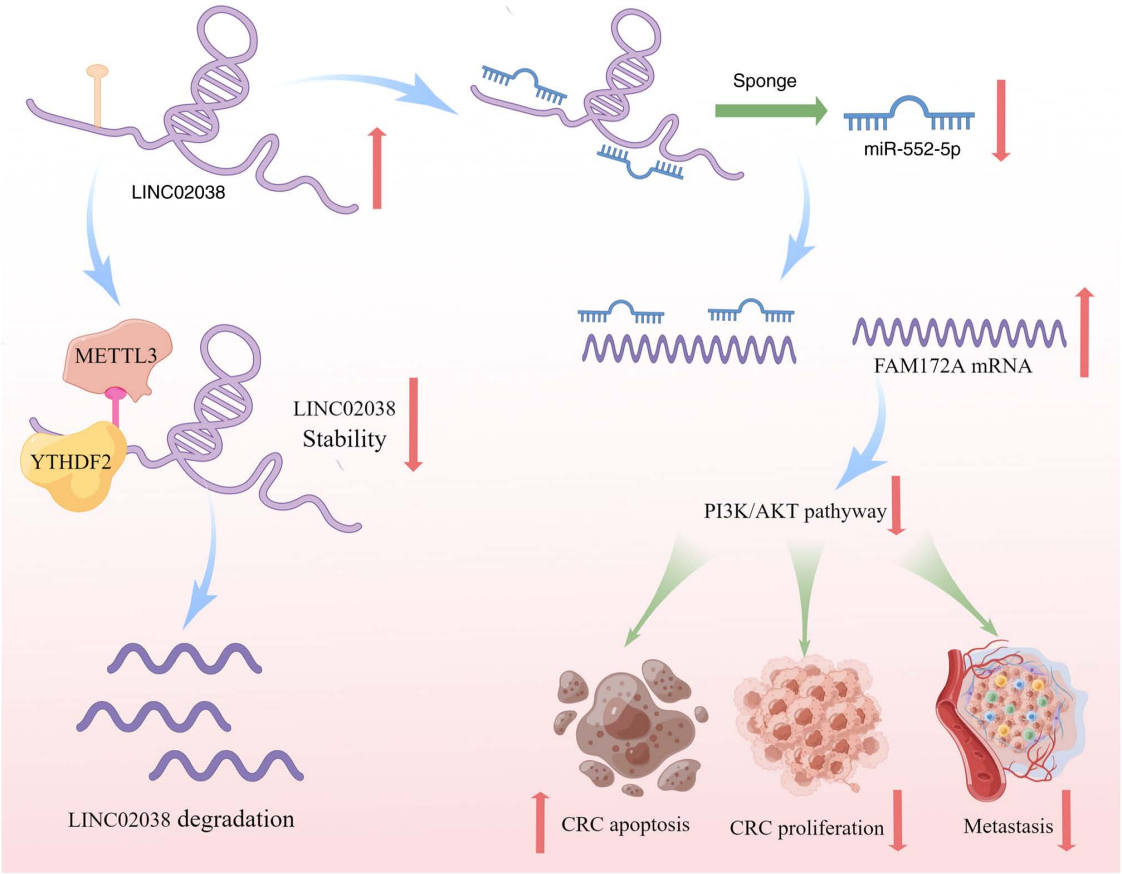

Figure 9. Graphic illustrating the m^{6}A-dependent effects of the LINC02038/miR-552-5p/FAM172A/PI3K/AKT regulatory loop on CRC growth. m^{6}A, N6-methyladenosine; CRC, colorectal cancer; miR, microRNA.

example, FAM172A inhibited CRC proliferation and invasion by being regulated at the post-transcriptional level by miR-27a via NF-κB pathways (34). Chen *et al* (35) reported that FAM172A was downregulated in human pancreatic cancer tissues and inhibited epithelial-mesenchymal transition (EMT) in pancreatic cancer cells via MAPK/ERK and PI3K/Akt signaling.

In the present study, overexpression of LINC02038 partly rescued the effects of FAM172A silencing on malignant phenotypes of CRC cells, suggesting that FAM172A is essential for the biological effects mediated by the LINC02038/miR-552-5p axis in CRC cells. Emerging evidence reveals that RNA methylation plays a crucial role in the dysfunction of lncRNAs (36). The most prevalent type of RNA modification is m^{6}A modification (37,38). The present study aimed to determine whether m^{6}A modification sites existed in the LINC02038 sequence. Notably, several sites with high confidence for m^{6}A modification were found on LINC02038. Therefore, it was hypothesized that abnormal expression of LINC02038 may be linked to m^{6}A modification. RNA pull-down experiments showed that LINC02038 specifically binds to METTL3 and YTHDF2. METTL3, an m^{6}A writer RNA methyltransferase, was upregulated in CRC and regulated mRNA stability (39). Knockdown of METTL3 enhanced LINC02038 expression in this study, rendering LINC02038 incapable of m^{6}A modification due to METTL3 deficiency. Furthermore, the m^{6}A reader YTHDF2 has been implicated in regulating methylated mRNA stability and tumor progression in CRC (40,41). The present study found that YTHDF2 directly bound to specific m^{6}A sites on LINC02038 and regulated it in an m^{6}A-dependent manner. The results confirmed elevated expression of YTHDF2 in CRC and its regulatory effect on LINC02038 instability to promote CRC.

In summary, the present study demonstrated that LINC02038 is a novel tumor suppressor in CRC. Decreased levels of LINC02038 in CRC patients were associated with increased tumor metastasis and worse survival due to m^{6}A modification. LINC02038 sponged miR-552-5p to impede CRC development, which was mediated by FAM172A and PI3K/Akt signaling in CRC cells. These results shed new light on the mechanisms underlying the function of the LINC02038 in CRC. Therefore, m^{6}A modification of the LINC02038/miR-552-5p/FAM172A axis may represent a promising therapeutic approach and prognostic biomarker for CRC (Fig. 9).

Acknowledgements

Not applicable.

Funding

The present study was funded by the Natural Science Foundation of Guangdong Province (grant no. 2018A0303130312), the clinical characteristic technology project of Guangzhou (grant no. 2023C-TS45).

Availability of data and materials

The datasets used and/or analyzed during the present study are available from the corresponding author on reasonable request.

Authors' contributions

WL, ZZ and CY conceived and designed the present study. WL, ZZ and JL performed the experiments. XL and BH acquired and collected tissue samples and the clinical data. KQ and ZM performed the *in vivo* experiments. JD and WL analyzed and interpreted the data. WL and ZZ wrote the manuscript. CY edited the manuscript. WL and JD confirm the authenticity of all the raw data. All authors read and approved the final manuscript.

Ethics approval and consent to participate

The present study involving human tissues was approved by the Ethics Committee of the First People's Hospital of Foshan, Guangdong (approval no. AF-SOP-18-1.6-2). All patients provided written informed consent prior to their inclusion within the study. All animal experiments were approved by the Committee of the Ethics of Animal Experiments of Southern Medical University (approval no. 2032101).

Patient consent for publication

Not applicable.

Competing interests

The authors declare that they have no competing interests.

References

1. Kanth P and Inadomi JM: Screening and prevention of colorectal cancer. BMJ 374: n1855, 2021.
2. Dekker E, Tanis PJ, Vleugels JLA, Kasi PM and Wallace MB: Colorectal cancer. Lancet 394: 1467-1480, 2019.
3. Biller LH and Schrag D: Diagnosis and treatment of metastatic colorectal cancer: A review. JAMA 325: 669-685, 2021.
4. Sung H, Ferlay J, Siegel RL, Laversanne M, Soerjomataram I, Jemal A and Bray F: Global cancer statistics 2020: GLOBOCAN estimates of incidence and mortality worldwide for 36 cancers in 185 countries. CA Cancer J Clin 71: 209-249, 2021.
5. Li N, Lu B, Luo C, Cai J, Lu M, Zhang Y, Chen H and Dai M: Incidence, mortality, survival, risk factor and screening of colorectal cancer: A comparison among China, Europe, and northern America. Cancer Lett 522: 255-268, 2021.
6. Zhou L, Zhu Y, Sun D and Zhang Q: Emerging roles of long non-coding RNAs in the tumor microenvironment. Int J Biol Sci 16: 2094-2103, 2020.
7. Chi Y, Wang D, Wang J, Yu W and Yang J: Long non-coding RNA in the pathogenesis of cancers. Cells 8: 1015, 2019.
8. Zhao Z, Sun W, Guo Z, Zhang J, Yu H and Liu B: Mechanisms of lncRNA/microRNA interactions in angiogenesis. Life Sci 254: 116900, 2020.
9. Winkle M, El-Daly SM, Fabbri M and Calin GA: Noncoding RNA therapeutics - challenges and potential solutions. Nat Rev Drug Discov 20: 629-651, 2021.
10. Chan JJ and Tay Y: Noncoding RNA: RNA regulatory networks in cancer. Int J Mol Sci 19: 1310, 2018.
11. Tang J, Yan T, Bao Y, Shen C, Yu C, Zhu X, Tian X, Guo F, Liang Q, Liu Q, *et al*: LncRNA GLCC1 promotes colorectal carcinogenesis and glucose metabolism by stabilizing c-Myc. Nat Commun 10: 3499, 2019.
12. Lin X, Zhuang S, Chen X, Du J, Zhong L, Ding J, Wang L, Yi J, Hu G, Tang G, *et al*: lncRNA ITGB8-AS1 functions as a ceRNA to promote colorectal cancer growth and migration through integrin-mediated focal adhesion signaling. Mol Ther 30: 688-702, 2022.
13. Hu XT, Xing W, Zhao RS, Tan Y, Wu XF, Ao LQ, Li Z, Yao MW, Yuan M, Guo W, *et al*: HDAC2 inhibits EMT-mediated cancer metastasis by downregulating the long noncoding RNA H19 in colorectal cancer. J Exp Clin Cancer Res 39: 270, 2020.
14. Chen J, Song Y, Li M, Zhang Y, Lin T, Sun J, Wang D, Liu Y, Guo J and Yu W: Comprehensive analysis of ceRNA networks reveals prognostic lncRNAs related to immune infiltration in colorectal cancer. BMC Cancer 21: 255, 2021.
15. Karreth FA and Pandolfi PP: ceRNA cross-talk in cancer: When ce-bling rivalries go awry. Cancer Discov 3: 1113-1121, 2013.
16. Xu AM, He CJ, Tuerxun Z and Anikezi A: FAM172A affects cell proliferation and apoptosis not by targeting β-tubulin in HepG2 cells. Transl Cancer Res 9: 5637-5644, 2020.
17. Narayanankutty A: PI3K/Akt/mTOR pathway as a therapeutic target for colorectal cancer: A review of preclinical and clinical evidence. Curr Drug Targets 20: 1217-1226, 2019.
18. Vu LP, Cheng Y and Kharas MG: The biology of m^6A RNA methylation in normal and malignant hematopoiesis. Cancer Discov 9: 25-33, 2019.
19. Ianniello Z, Paiardini A and Fatica A: N^6-Methyladenosine (m^6A): A promising new molecular target in acute myeloid leukemia. Front Oncol 9: 251, 2019.
20. Xiang S, Liang X, Yin S, Liu J and Xiang Z: N6-methyladenosine methyltransferase METTL3 promotes colorectal cancer cell proliferation through enhancing MYC expression. Am J Transl Res 12: 1789-1806, 2020.
21. Livak KJ and Schmittgen TD: Analysis of relative gene expression data using real-time quantitative PCR and the 2(-Delta Delta C(T)) method. Methods 25: 402-408, 2001.
22. Li HB, Tong J, Zhu S, Batista PJ, Duffy EE, Zhao J, Bailis W, Cao G, Kroehling L, Chen Y, *et al*: m^6A mRNA methylation controls T cell homeostasis by targeting the IL-7/STAT5/SOCS pathways. Nature 548: 338-342, 2017.
23. Pfaff J, Hennig J, Herzog F, Aebersold R, Sattler M, Niessing D and Meister G: Structural features of Argonaute-GW182 protein interactions. Proc Natl Acad Sci USA 110: E3770-E3779, 2013.
24. Hicks JA, Li L, Matsui M, Chu Y, Volkov O, Johnson KC and Corey DR: Human GW182 paralogs are the central organizers for RNA-mediated control of transcription. Cell Rep 20: 1543-1552, 2017.
25. Smolarz B, Zadrożna-Nowak A and Romanowicz H: The Role of lncRNA in the development of tumors, including breast cancer. Int J Mol Sci 22: 8427, 2021.
26. Ghafouri-Fard S, Abak A, Tondro Anamag F, Shoorei H, Majidpoor J and Taheri M: The emerging role of non-coding RNAs in the regulation of PI3K/AKT pathway in the carcinogenesis process. Biomed Pharmacother 137: 111279, 2021.
27. He Q, Long J, Yin Y, Li Y, Lei X, Li Z and Zhu W: Emerging roles of lncRNAs in the formation and progression of colorectal cancer. Front Oncol 9: 1542, 2019.
28. Statello L, Guo CJ, Chen LL and Huarte M: Gene regulation by long non-coding RNAs and its biological functions. Nat Rev Mol Cell Biol 22: 96-118, 2021.
29. Smillie CL, Sirey T and Ponting CP: Complexities of post-transcriptional regulation and the modeling of ceRNA crosstalk. Crit Rev Biochem Mol Biol 53: 231-245, 2018.
30. Yang XZ, Cheng TT, He QJ, Lei ZY, Chi J, Tang Z, Liao QX, Zhang H, Zeng LS and Cui SZ: LINC01133 as ceRNA inhibits gastric cancer progression by sponging miR-106a-3p to regulate APC expression and the Wnt/β-catenin pathway. Mol Cancer 17: 126, 2018.
31. Xu M, Chen X, Lin K, Zeng K, Liu X, Xu X, Pan B, Xu T, Sun L, He B, *et al*: lncRNA SNHG6 regulates EZH2 expression by sponging miR-26a/b and miR-214 in colorectal cancer. J Hematol Oncol 12: 3, 2019.
32. Chen T, Lei S, Zeng Z, Zhang J, Xue Y, Sun Y, Lan J, Xu S, Mao D and Guo B: Linc00261 inhibits metastasis and the WNT signaling pathway of pancreatic cancer by regulating a miR-552-5p/FOXO3 axis. Oncol Rep 43: 930-942, 2020.
33. Cai W, Xu Y, Yin J, Zuo W and Su Z: miR-552-5p facilitates osteosarcoma cell proliferation and metastasis by targeting WIF1. Exp Ther Med 17: 3781-3788, 2019.
34. Liu W, Qian K, Wei X, Deng H, Zhao B, Chen Q, Zhang J and Liu H: miR-27a promotes proliferation, migration, and invasion of colorectal cancer by targeting FAM172A and acts as a diagnostic and prognostic biomarker. Oncol Rep 37: 3554-3564, 2017.

35. Chen Y, Liu P, Shen D, Liu H, Xu L, Wang J, Shen D, Sun H and Wu H: FAM172A inhibits EMT in pancreatic cancer via ERK-MAPK signaling. Biol Open 9: bio048462, 2020.
36. Liu HT, Zou YX, Zhu WJ, Sen-Liu, Zhang GH, Ma RR, Guo XY and Gao P: lncRNA THAP7-AS1, transcriptionally activated by SP1 and post-transcriptionally stabilized by METTL3-mediated m6A modification, exerts oncogenic properties by improving CUL4B entry into the nucleus. Cell Death Differ 29: 627-641, 2022.
37. Deng X, Su R, Weng H, Huang H, Li Z and Chen J: RNA N^6-methyladenosine modification in cancers: Current status and perspectives. Cell Res 28: 507-517, 2018.
38. Roundtree IA, Evans ME, Pan T and He C: Dynamic RNA modifications in gene expression regulation. Cell 169: 1187-1200, 2017.
39. Peng W, Li J, Chen R, Gu Q, Yang P, Qian W, Ji D, Wang Q, Zhang Z, Tang J and Sun Y: Upregulated METTL3 promotes metastasis of colorectal cancer via miR-1246/SPRED2/MAPK signaling pathway. J Exp Clin Cancer Res 38: 393, 2019.
40. Zhou D, Tang W, Xu Y, Xu Y, Xu B, Fu S, Wang Y, Chen F, Chen Y, Han Y and Wang G: METTL3/YTHDF2 m6A axis accelerates colorectal carcinogenesis through epigenetically suppressing YPEL5. Mol Oncol 15: 2172-2184, 2021.
41. Liu W, Liu C, You J, Chen Z, Qian C, Lin W, Yu L, Ye L, Zhao L and Zhou R: Pan-cancer analysis identifies YTHDF2 as an immunotherapeutic and prognostic biomarker. Front Cell Dev Biol 10: 954214, 2022.